Published in final edited form as:
J Phys Chem B. 2014 March 27; 118(12): 3281–3290. doi:10.1021/jp4102916.

On the potential of hyperpolarized water in biomolecular NMR studies

Talia Harris, **Or Szekely**, and **Lucio Frydman***
Chemical Physics Department, Weizmann Institute of Science, Rehovot, Israel

Abstract

A main obstacle arising when using *ex-situ* hyperpolarization to increase the sensitivity of biomolecular NMR, is the fast relaxation that macromolecular spins undergo upon being transferred from the polarizer to the spectrometer where their observation takes place. To cope with this limitation the present study explores the use of hyperpolarized water, as a means to enhance the sensitivity of nuclei in biomolecules. Methods to achieve proton polarizations in excess of 5% in water transferred into the NMR spectrometer were devised, as were methods enabling this polarization to last for up to 30 sec. Upon dissolving aminoacids and polypeptides sited at the spectrometer into such hyperpolarized water, a substantial enhancement of certain biomolecular amide and amine proton resonances was observed. This exchange driven ^{1}H enhancement was further passed on to sidechain and to backbone nitrogens, owing to spontaneous one-bond Overhauser processes. ^{15}N signal enhancements >500 over 11.7 T thermal counterparts could thus be imparted, in a kinetic process that enabled multi-scan signal averaging. Besides potential bioanalytical uses, this approach opens interesting possibilities in the monitoring of dynamic biomolecular processes -including solvent accessibility and exchange process.

Keywords

nuclear magnetic resonance; dynamic nuclear polarization; hyperpolarized water; biomolecular spectroscopy; sensitivity enhancement

1 Introduction

Recent developments in high-field dynamic nuclear polarization (DNP), can greatly enhance the sensitivity of nuclear magnetic resonance (NMR) in solids and liquids.1–8 Most promising among these methods, particularly within the context of solution-phase NMR spectroscopy and imaging (MRI), is the dissolution DNP approach. Dissolution DNP improves NMR's sensitivity by executing the nuclear hyperpolarization *ex situ,* on a custom polarizer where the targeted sample is co-mixed with a stable (often organic) radical, and cooled into an amorphous frozen glass.9 After exposing such cryogenic system to suitable microwave radiation, the very high polarization of the electron spins (≥90%) is efficiently transferred to the surrounding nuclei in bulk. This microwave-driven polarization transfer happens over minutes or hours at $T \leq 1.5$ K; the sample is subsequently returned to the

* lucio.frydman@weizmann.ac.il, Tel. +972-8-934-4903.

Europe PMC Funders Author Manuscripts

liquid state by exposing it to hot vapors, and the resulting liquid is then flushed from the polarizer into the NMR/MRI probe/coil for a rapid inductive-based detection10. This *ex situ* method can create nuclear polarizations in excess of 30%,11–17 and for the case of small molecules its sudden-dissolution nature can preserve much of these earnings for subsequent liquid-phase NMR observations. Such sensitivity gains can be truly outstanding, akin to years of non-stop conventional signal averaging18–20. Still, when considering the use of this setup for biomolecular applications, a serious limitation arises. This derives from the short relaxation times that characterize biomolecules, particularly in the very low (<0.1 T) magnetic fields that the dissolved sample has to negotiate between the polarizer and the spectrometer. Indeed relaxation rates in excess of a kHz are typical of medium-sized biomolecules tumbling with ns correlation times,21–23 implying that in the 1-3 sec timescales that the dissolution DNP method requires for the sample to traverse through a low-field region, most of the hard-earned polarization gains will be lost. The sample hyperpolarization will be further depleted by the additional relaxation induced by the paramagnetic polarizing agent, which gets dissolved and transferred together with the targeted sample into the NMR spectrometer.

A number of alternatives have emerged over recent years to deal with this limitation. Most general among these solutions is arguably the proposal by Kockenberger et al,24 which employs a dual-magnet approach whereby the solid sample is transported from an upper DNP magnet into a lower NMR magnet where samples are melted and observed. While also in this setup the sample transverses a low-field region in-between the magnets it does so as a cryogenic pellet, opening an opportunity for preserving the hyperpolarization of even large biomolecules thanks to their cryogenic state. In a scheme that follows more closely the original *ex situ* DNP setup, Hilty and coworkers have recently described a dissolution device that maximizes sample transport speed while minimizing turbulence through a system of back-pressure regulation.25,26 Using this system and a modified Hypersense polarizer a total sample dissolution-to-NMR delay of 1.2 s was achieved; short enough to endow the original *ex situ* approach with 300-3000× sensitivity gains for certain ^{13}C sites in perdeuterated, unfolded polypeptides.20 Yet another interesting option recently demonstrated within the context of DNP-enhanced biomolecular NMR, focuses the hyperpolarization on perdeuterated ^{15}N-labeled systems, which were allowed to slowly exchange their deuterons with protons of water acting as dissolution solvent.27 As this H/D exchange process takes place once the sample has reached the high-field NMR magnet and probe, the ^{15}N sensitivity enhancement is preserved and can be passed onwards to protons.

The present study examines an alternative way to cope with these limitations, that uses hyperpolarized water as a mean to enhance the sensitivity of biomolecular nuclei. We find that water protons could be spin-aligned rapidly in a cryogenic DNP setup, delivering polarizations of ≈5% after their dissolution and transfer to the NMR scanner. This enhancement could be made relatively long-lived, thanks to extended relaxation times T_1 realized by gentle heating and by adding a co-solvent that executed a post-melting radical extraction. Even factoring all dilution and relaxation losses, the ensuing method led to magnetizations that where over 100× larger than thermal counterparts involving pure water placed in a high field magnet. Upon using this hyperpolarized water to dilute a biomolecule waiting in the NMR spectrometer, a number of amine and amide groups underwent rapid

exchange of their protons with H_2O, leading to a clear enhancement of their ^1H resonances. This incorporation of hyperpolarized protons also led to an Overhauser-driven heteronuclear effect, whereby ^{15}N sites that were chemically bound to solvent-exchanging protons underwent a spontaneous magnetization enhancement. ^{15}N signal enhancements equating to hundreds of times the thermal equilibrium ^{15}N polarization could thus be recorded for both backbone and sideband amide and amine sites; these effects could last over significant times, opening the possibility of exploiting them in mutli-scan acquisitions. Besides enabling new bioanalytical capabilities via their sensitivity enhancements, this kind of experiment opens new opportunities to monitor dynamic biomolecular processes involving water H-exchange as reporter –including studies of protein folding and solvent accessibility.

2 Materials and Methods

Dynamic Nuclear Polarization

Water hyperpolarization was achieved by dissolving 25 mM of TEMPO radical (Sigma Aldrich, St. Louis, MO) in a 1.5:1 H_2O:glycerol (v/v) solution. Samples –usually of 150 μL or less– were hyperpolarized in an Oxford Instruments (Tubney Woods, Abingdon, UK) Hypersense® 3.35 T polarizer operating at 1.5 K, by irradiating a co-frozen TEMPO radical with ≤180 mW at ~94.1 GHz. Following DNP samples were dissolved in 99.9% D_2O (Sigma Aldrich) and heptane (Sigma Aldrich) as specified in the text, and transferred to the NMR by a 10 bar pulse of pressurized helium gas applied over 1.5 seconds. ^1H dilution factors in these dissolution DNP experiments were determined by measuring the absorbance of equivalent samples containing known quantities of dissolved red food coloring; these are reported for various conditions in Table 1 of the Supplementary Information. The absorbance values in the latter samples were measured on an Ultrospec 2100pro UV/Visible spectrophotometer (Amersham Biosciences, Piscataway, NJ) at a 492 nm wavelength, using a 17.8 MΩ·cm H_2O sample as blank.

Sample preparation

For the exchangeable ^1H NMR experiments (Figure 4), a concentrated sample of partially deuterated arginine was prepared by dissolving this amino acid at natural abundance and in powdered form (≥98% pure, Sigma Aldrich, St. Louis, MO) in 99.9% D_2O (Sigma Aldrich, St. Louis, MO), adjusting the pH to ~3 with concentrated HCl, and drying it by rotary evaporation. The procedure was repeated and the remaining powder was dissolved in 3 mL 99% D_2O to a final concentration of 1 M. This arginine sample was inserted into the 10 mm NMR tube subsequently used in the hyperpolarized water injection experiments. For the water-derived ^{15}N enhancement experiments of small molecules (Figures 5 and 6), sample volumes and concentrations included: 500 μL of 200 mM ^{15}N-urea (Cambridge Isotopes, Cambridge, MA), 350 μL of 500 mM ^{15}N-alanine (Cambridge Isotopes), and 0.7 mL of 2.1 M natural abundance arginine at pH~3 (Sigma Aldrich). All samples were prepared in 99.9% D_2O, and analyzed in 10 mm NMR tubes. Finally, for the water-derived ^{15}N enhancement experiments of biomolecules (Figure 7), modified aldehyde reductase (40 kDa) was cloned into pET28_TEVH and expressed in BL21 (DE3) bacteria using 4 L of M9 minimal media supplemented with ^{15}N labeled ammonium chloride. The bacterial lysate was applied to a Ni column (HisPrep FF 16/10, GE Healthcare Biosciences, Uppsala,

Europe PMC Funders Author Manuscripts

Sweden) and eluted with imidazole to yield a partially purified protein mix. The imidazole was removed by applying the protein mix to a preparative desalting column (HiPrep_26/10, GE Healthcare) equilibrated with phosphate buffered saline (PBS). The protein was filtered, 0.02% NaN_3 plus Trypsin were added to it, and the mixture was subsequently incubated overnight at 37 °C in order to digest the reductase. The ensuing polypeptide mix was then concentrated on a Centricon with a 10 kDa molecular weight cut off (Millipore, Billerica, MA). The flow-through contained peptides with a M_w <10 kDa which were subsequently removed from a Resource column (GE Healthcare) with 90% Acetonitrile and 0.1% TFA. The resulting mixture of polypeptides was frozen and lyophilized to obtain a dry powder. An ~11mg/mL solution was prepared by dissolving the powder in 97% D_2O buffer (25 mM KH_2PO_4, 50mM NaCl) and its pD was adjusted to ~10 with NaOH to ensure rapid hydrogen exchange.

NMR spectroscopy

NMR experiments were conducted in an 11.7 T Magnex magnet (Abingdon, Oxfordshire, UK) run by a Varian iNova console (Palo Alto, CA) and equipped with a QNP Bruker (Karlsruhe, Germany) 10 mm probe. NMR experiments were triggered upon dissolution and injection of the hyperpolarized water sample into the NMR tubes waiting with their samples inside the magnet bore. All NMR data were processed using Matlab® software (The MathWorks Inc, Natick, MA) using an exponential decay as a line-broadening function, and when needed peaks were fitted as Lorentzians using Dmfit (The Comfit Consortium, Orleans, France).28

3 Results

Hyperpolarizing water

Dissolution DNP studies have shown that water samples containing 10-40 mM of a nitroxide radical mixed with the appropriate proportion of glassing agent can be efficiently polarized when irradiated by microwaves at $T \leq 1.5$ K in high magnetic fields.18,29,30 Figure 1 illustrates the build-up behavior for this microwave-driven water polarization, as measured by the liquid state enhancement observed after dissolving a sample polarized in a 3.35T Hypersense, with 3 mL D_2O. This curve evidences a 10±2 min characteristic buildup time for the solid-state polarization; in terms of the achievable post-dissolution enhancement, such optimized hyperpolarization conditions led to signals decaying ≈1000-fold as they reach thermal equilibrium in the 11.7 T NMR used in this study (Fig. 1, inset).

Although very promising, such enhancement figures are deceptively high. Comparisons between a hyperpolarized and a thermal signal measure relative enhancements, but ignore the ^1H signal reduction due to the dilution of the hyperpolarized water with the glassing agent needed for an effective cryogenic DNP process, or the substantial dilution with non-polarized solvent that the hyperpolarized sample undergoes upon melting and flushing it across the two magnets. In order to address the first of these concerns, we used glycerol as water's co-glassing agent. Glycerol was chosen over other possible co-solvents, given this compound's relatively high concentration of exchangeable protons. These will be polarized as well by the solids DNP process, and eventually contribute to the pool of exchangeable

protons whose hyperpolarization one aims to transfer to the biomolecule. At a 3:2 water:glycerol v/v ratio the ensuing sample polarized efficiently, and still delivered ~76% of the exchangeable protons expected from a pure water counterpart. To address the second concern, we attempted to decrease the dilution factor by increasing the volume of hyperpolarized sample –without a concomitant increase in the volume of the dissolution solvent. While the water's dilution could be reduced by a factor of ≈10 in this fashion, this came at the cost of severely reducing the T_1 of the hyperpolarized water. This penalty reflects the fact that all efforts aimed at reducing a pellet's dilution, will *de facto* increase the nitroxide's post-dissolution concentration; since this radical efficiently polarizes the protons but is also an effective water T_1 relaxation agent, particularly in the low magnetic fields experienced by H_2O during its transfer from the polarizer to the NMR magnet,31,32 the net hyperpolarization achievable from these reduced-volume solutions actually drops. In order to reduce water's post-DNP dilution without decreasing the T_1 of the hyperpolarized ^1H_S, a number of alternatives were tested. Most efficient among these ended up being the combined use of immiscible organic and aqueous solvents to melt and transfer the hyperpolarized water pellet.30 This method reduces the dilution factor thanks to the phase separation that the immiscible organic solvent will undergo after the sample is transfered, as it settles outside the NMR observation coil region. At the same time, a suitable organic phase can efficiently extract the organic co-polarizing TEMPO radical over the course of the sample-transfer process, thereby decreasing the aqueous phase relaxivity. Heptane was found as a useful co-solvent for achieving these dual goals, without introducing substantial susceptibility-derived distortions in the ensuing lineshapes. Typically, 150 μL of hyperpolarized water samples were thus dissolved and transferred with a 1.5/3 mL mix of water/heptane, leading to a net dilution factor of ≈8. Further reductions in the aqueous' phase dissolution volumes did not significantly reduce the hyperpolarized pellet's dilution factor.

Given the importance of maximizing T_1s for the sake of minimizing polarization losses in the case of fast-relaxing nuclei like ^1Hs, two additional provisions were adopted. First, in all our experiments D_2O was used as the aqueous dissolution phase; by relying on this deuterated solvent, a ca. four-fold increase in the T_1 of the hyperpolarized water protons was observed. In addition, the tube transferring the dissolved hyperpolarized water between the DNP and the NMR magnets, as well as the NMR probe itself, were preheated to ca. 40-50 °C; this lead to an additional lengthening of the hyperpolarized ^1H's lifetimes. Numerous other precautions were assessed in the hope of further increasing the protons' T_1s –including the surrounding of the transfer line with ≈1000 G magnets along its ca. 2 m route, and solvent degassing. Yet these lead to negligible enhancements, and their use was thus discontinued. Table 1 in the Supplementary Information gives further quantitative data on how each of the processes described in this paragraph, assisted in achieving an enhanced water hyperpolarization at the NMR probe position.

The outcome of these efforts is summarized by the post-dissolution traces in Figure 2. This compares results obtained for a dissolution employing solely D_2O, with those stemming from a joint D_2O/heptane dissolution mix incorporating heating of the transfer line. The stronger, longer-lasting enhancements afforded by all the aforementioned steps are clearly evidenced; unfortunately, so are the significant radiation damping effects that highly

polarized water at these fields and concentrations are bound to lead to. These are reflected in both severe shifts and broadenings immediately upon dissolution, which decay as the hyperpolarization dies down. Still, judging by the areas of these small pulse-angle (<1°) experiments, optimal cases led to a polarization ≥5.2% and a $T_1 \geq 18$ sec. When contemplating the use of such polarization as source for enhancing the sensitivity of additional molecules, this performance should be further scaled by a ≈1/8 dilution factor associated with the sample's dissolution, and a 0.76 factor reflecting the decrease in labile protons owing to the use of the glycerol. All these factors combined still lead to a ≥120× enhancement over the polarization that is present in a pure water tube polarized in a 1 GHz NMR spectrometer –not an insignificant gain, that compares favorably to absolute ^{1}H water enhancements of approximately 15× obtained at 4.7 T by conventional dissolution DNP,29 and of approximately -10× obtained at 1.5 T by liquid state continuous-flow DNP.33

Sensitivity enhancement of exchangeable protons in small biomolecules

With these gains at hand, the use of DNP-enhanced water protons towards the magnification of NMR signals arising from labile biomolecular protons, was explored. To this end we targeted protons possessing solvent exchange rates k_{ex} that are sufficiently slow in the NMR time scale to give distinct peaks in the ensuing ^{1}H spectrum, and at the same time sufficiently fast to accommodate significant gains for the above-mentioned hyperpolarized water T_1 times. As the ultimate goal is to exploit these exchange processes in biomolecules with significantly shorter T_1s than those of the hyperpolarized water, the investigated paradigm explored the gains in polarization achieved by biomolecules that were waiting in the NMR magnet/probe, and exchanged their labile protons with those of water that was suddenly injected following dissolution DNP. This approach would have the advantage that during the transfer process the polarization will decay with the longer T_1 of the water protons, and significant polarizations could be imparted even on species with short proton T_1s. To investigate under what conditions would this approach be beneficial, basic calculations were performed on the extent by which protons H_{ex} that are initially thermally polarized, will enhance their z-magnetizations $\langle H_{ex} \rangle_z$ by chemical exchange with hyperpolarized water. Assuming that the injected water hyperpolarization is much higher than its thermal (Th) counterpart (*i.e.,* that $\langle H_2O \rangle_z(0) \gg \langle H_2O \rangle_z(\mathrm{Th})$) and that $[H_2O] \gg [H_{ex}]$, these calculations follow from modified Bloch-McConnell equations34 and predict a time-dependent exchangeable proton magnetization:

$$\langle H_{ex} \rangle_z (t) \approx \langle H_2O \rangle_z (0) \cdot \frac{k_{ex}}{\left(k_{ex} + \frac{1}{T_1^{H_{ex}}} - \frac{1}{T_1^{H_2O}} \right)} \cdot e^{-\frac{t}{T_1^{H_2O}}} \left(1 - e^{-\left(k_{ex} + \frac{1}{T_1^{H_{ex}}} - \frac{1}{T_1^{H_2O}} \right) \cdot t} \right) \quad (1)$$

where the T_1's denote the spin-lattice relaxation delay of the species and k_{ex} their mutual exchange rate.

Plots of this equation for a variety of conditions are given in Fig. 3a. These show that the maximum magnetization achievable by the exchangeable protons will be relatively insensitive to $T_1^{H_{ex}}$, or even to the water T_1, but will be sensitive to the $T_1^{H_{ex}} \cdot k_{ex}$ product.

Importantly, not only can high levels of single-shot polarization be achieved in this manner for H_{ex} relative to the polarization arriving with the water protons, but by applying selective pulses on the exchangeable proton sites, the water polarization can be preserved and multiple scans with enhanced signal can be acquired from a single dissolution. For a 90° selective pulsing taking place at a constant repetition time TR, the polarization contributions to the exchangeable proton signals will be described by

$$\langle H_{ex}\rangle_z(t,TR) \approx \langle H_2O\rangle_z(0)\cdot\frac{k_{ex}}{\left(k_{ex}+\frac{1}{T_1^{H_{ex}}}-\frac{1}{T_1^{H_2O}}\right)}\cdot e^{-\frac{t}{T_{1,H_2O}}}\left(1-e^{-\left(k_{ex}+\frac{1}{T_1^{H_{ex}}}-\frac{1}{T_1^{H_2O}}\right)\cdot TR}\right) \quad (2)$$

As shown in Figure 3b for a variety of instances, substantial sensitivity increases can then be obtained for the exchangeable protons. This can also be important if attempting to acquire multidimensional spectra, or to follow a dynamic process. It follows as well from the last expression that although an increase in the water T_1 only leads to a slight increase in the initial H_{ex} magnetization, the achievable polarization enhancement of the exchangeable sites in a multi-scan experiment can be significantly increased by prolonging $T_1^{H_2O}$ (Figure 3c).

With these expectations as background, Figure 4 illustrates the gains that this procedure afforded when applied to arginine, a small molecule possessing multiple exchanging sites. This compound exhibits different $\mathbf{H^2O} \longleftrightarrow \mathbf{H}N$- exchange rates k_{ex} for the non-equivalent NH, NH_2 and NH_3 groups in the molecule, with strong pH and temperature dependencies.[35,36] The polarization buildup is thus different for each group but is in all cases significant. A train of acquisitions following a water-based dissolution DNP experiment allows one to obtain insight into the rates of hydrogen exchange of these sites with the solvent (Fig. 4a-b).

Heteronuclei signal enhancement

Interestingly, not only can exchangeable protons be polarized, but also heteronuclei directly bound to such exchangeable protons are *spontaneously* polarized by injection of hyperpolarized water. This is illustrated in Figure 5a, which demonstrates how polarization from DNP-enhanced water ^{1}Hs migrates to urea's ^{15}N, without the need for any ^{1}H pulsing. A train of low flip angle pulses on the ^{15}N channel evidences the slow buildup of urea's ^{15}N polarization, reaching a maximum at ≈40 sec. The decay of this polarization is also slow, reflecting a T_1^N that for urea in a partly deuterated solution like the one arising in this case, is on the order of minutes. A number of factors are involved in this build-up/decay function, including the rate of amide/water ^{1}H exchange k_{ex}, the rate of ^{1}H-^{15}N cross-relaxation k_{NOE} driving the heteronuclear polarization transfer within urea, and the rates of polarization decay given by the ^{1}H T_1's of the water and urea sites as well as by the ^{15}N's own T_1. Three-site exchange simulations (Supporting Information) show that the magnitude of the ^{15}N enhancement will depend in a complex fashion on these multiple factors. Still, fits of the experimental data based on this model reveal that the heteronuclear Overhauser transfer

k_{NOE} is the rate determining step of this $^{1}H_{water} \xrightarrow{k_{ex}} {}^{1}H_{ex} \xrightarrow{k_{NOE}} {}^{15}N$ polarization transfer process. With this knowledge at hand, one can propose a simpler two-site model whereby the observable ^{15}N magnetization only arises from a ^{1}H reservoir made available by the DNP experiment. As this is left unperturbed apart from its relaxation back to equilibrium, the ^{15}N polarization's time evolution can be described by37:

$$\frac{d}{dt}\begin{bmatrix} \langle H_Z \rangle (t) \\ \langle N_Z \rangle (t) \end{bmatrix} = \begin{bmatrix} -\frac{1}{T_1^H} & 0 \\ k_{^1H \rightarrow {}^{15}N} & -\frac{1}{T_1^{N,eff}} \end{bmatrix} \begin{bmatrix} \langle H_Z \rangle (t) \\ \langle N_Z \rangle (t) \end{bmatrix}, \quad (3)$$

where $k_{^1H \rightarrow {}^{15}N}$ summarizes the average effects of the $H_2O \rightarrow {}^{15}N$ process, and $T_1^{N,eff}$ is a decay time factoring both the natural T_1 of the ^{15}N as well as the depleting effects of the pulses used to interrogate the signal.

The enveloping line in Figure 5 shows a fit of this simplified model to traces arising from this kind of experiment, leading to an effective rate $k_{^1H \rightarrow {}^{15}N} = 0.29 \pm 0.02$ sec^{-1}, and times $T_1^{N,eff} \approx 89.2\ sec, T_1^H \approx 16$ sec. By setting $\frac{d}{dt}[\langle N_Z \rangle (t)]_{t=t_{max}}$ to zero, this model also let's one find the approximate time leading to the maximal ^{15}N enhancement: $t_{max} = 34$ sec. For an initial degree of maximal ^{1}H polarization injected in the reservoir the solution of eq. (3) also predicts a maximum achievable ^{15}N polarization that from the parameters fitted in Figure 5 should be ≈344×, close to the experimentally observed value of 320× (Figure 5, inset).

Figure 6 illustrates an application of this strategy to the enhancement of ^{15}N sites in alanine and arginine. For alanine, a similar analysis as the one just described suggests a maximal ^{15}N sensitivity enhancement ca. 40 sec after sample injection, although with a polarization enhancement of ≈180×. A similar experiment on a 0.7 M D_2O solution of natural abundance arginine at pD≈3 shows a maximum enhancement at ≈20 sec with the $^{15}NH_2$ and $^{15}NH_3$ sites showing: ≈360× and ≈280× levels of enhancement, respectively. Much lower enhancements (≈50x) are observed for the NH site, due to its slower rate of hydrogen exchange. Noteworthy, as the hydrogen exchange with water for the former two arginine sites is fairly rapid, it is not necessary to wait a relatively long T_1 delay to obtain the optimum enhancement: multiple scans collected at times $\approx (k_{ex})^{-1}$ lead to significantly enhanced signals which can be averaged over several repeated scans (Fig. 6c). A similar approach could proof useful in the acquisition of Hadamard-encoded or sparsely-sampled 2D NMR spectra.

In order to investigate whether these initial observations can be extended to larger biomolecules, the heteronuclear transfer experiment was applied on a lysate of ^{15}N-labeled aldehyde reductase. Trypsin-based lysis reduced the original 40 kDa M_W of this well-folded protein into an array of peptides of mostly $M_W \approx 3$ kDa, with some 5% reaching up to the 10 kDa molecular weight cut-off used. It can be assumed that the peptides in this mixture do not contain residual structure and that their chains are fully extended. These conditions should favor a rapid exchange of their amine and amide N**H**'s with the hyperpolarized water

protons. To examine what kind of effective ^{15}N signal enhancement this could lead to, a series of ^{15}N NMR spectra where collected using 90° excitation pulses following the injection of hyperpolarized water. These results are shown in Figure 7a, and confirm a sensitivity enhancement of both backbone amide and side-chain amine resonances. The build-up of these signals is relatively rapid, as expected for the high k_{ex} rates characterizing these unfolded peptides. The apparent decay of the signal enhancement by contrast, 20±1 sec, is much slower than the overall relaxation of the backbone amides, whose global T_1^N is 1.8±0.8 sec. This relatively slow decay reflects the T_1 of the hyperpolarized water protons, that support the ^{15}N repolarization process between consecutive ^{15}N scan. These long lifetimes allows one to achieve an ^{15}N enhancement beyond what would be possible with a single acquisition; comparing a sum of scans collected over a 25 sec period (Figure 7b, upper trace) against a thermal equilibrium ^{15}N spectrum (Figure 7b, middle trace), indicates that most peaks in the amide backbone region can be enhanced in this multi-scan fashion by > 500×. A similar enhancement characterizes ^{15}N sites in the NH_3 region, as well as arginine's guanidine ^{15}N sites in the lysate. The only amide nitrogens that do not appear enhanced are those belonging to proline groups, owing to their lack of exchangeable protons.

4 Discussion and Conclusions

Bringing the benefits of DNP to bear onto the study of biomolecules in solution, is an important challenge of contemporary NMR. The present work investigated a way of bypassing the T_1 bottleneck that slowly-tumbling biomacromolecules will face upon transferring from the DNP to the NMR fields, based on an *ex situ* hyperpolarization of water and subsequent exchange-driven transfers of polarization to labile biomolecular sites. Although addressing a small subset of all sites, such an efficient enhancement of exchangeable protons –and of their bonded nitrogens - could facilitate a wide variety of studies currently supported, *inter alia*, by ^1H-^{15}N 2D correlations. This strategy's success depends on maximizing the absolute polarization of the H_2O achieved in the cryogenic solid, minimize the dilution that the cryogenic pellet will undergo upon melting and shuttling, and reduce the ^1H relaxation losses that limit the time over which the H_2O polarization can be exploited in the biomolecular analyses. The present study placed an emphasis on optimizing the last two of these aspects, with dilution and relaxation losses minimized by a combination of dissolution and transfer precautions. With these provisions dilution penalties were limited to ≈90% –still a non-negligible factor liable to improvement – and relaxation times reached 15 - 20 sec. All this lead to a nearly ≈100× enhancement over the polarization characterizing a tube of pure water placed in a high field system. Even further room for enhancement remains in terms of optimizing the cryogenic solid-state polarization, as witnessed by the fact that electrons are over 90% polarized in the DNP setup used whereas the ^1H polarization hardly cleared the 5% mark.

Even with these limitations, an interesting aspect of the examined approach lies in its ability to spontaneously enhance the resonances of ^{15}N attached to labile protons, by factors in the 100-1000× range. These results are particularly promising for ^{15}N sites that undergo rapid ^1H exchange, e.g. Lysine side chains and amide positions in unstructured proteins at

high pH; these sites cannot be efficiently enhanced by INEPT-like sequences, while thermal equilibrium $^{1}H \rightarrow ^{15}N$ NOE methods are inefficient in macromolecules. The spontaneous nature of the transfer is also promising for human-oriented NMR imaging setups, which are rarely equipped with full double-resonance irradiation capabilities. It is conceivable, however, that a more active INEPT-like transfer might be more effective for N-H sites undergoing intermediate proton exchange than the spontaneous transfer assayed in this study. We have carried out such tests, but preliminary results indicate that this strategy is challenged if attempting to leave the radiation-broadened reservoir of hyperpolarized H_2O untouched for the sake of performing multiple ^{15}N acquisitions. Further efforts aimed at clarifying these issues are ongoing.

The enhanced biomolecular sensitivity experiments demonstrated in this work were carried out on intrinsically unfolded systems liable to fast hydrogen exchange of their backbone protons. Additional potential targets could include structured polypeptides which are kept artificially unfolded in the NMR tube where their measurement will take place, until the arrival of hyperpolarized water triggers their sudden folding. Even in folded systems, sensitivity gains should arise from water accessible side-chains whose protons are rapidly exchanging with those of the hyperpolarized water. A different kind of experimental window that might be opened by the hyperpolarized experiments hereby described, involves measuring the rates of water exchange and/or water accessibility in biomolecules.38 Two kinds of water-proton exchange experiments are commonly used, depending on the range of exchange rates to be accessed. Slower exchange processes are usually determined by isotope dilution methods whereby the volumes of proton peaks in proteins whose exchangeable sites were fully deuterated, are monitored in real time as the sample is diluted by fully protonated water (or conversely, whereby peak decays are quantified as a fully protonated protein is diluted in deuterated water).39,40 Another method, better suited for studying more rapid exchange processes, relies on observing the decrease in the intensities of the labile peaks upon solvent water saturation/inversion. In this method the signal of the individual exchangeable proton sites will depend on k_{ex} as well as the site's T_1 value, and hence is limited to k_{ex} on the order of the site's T_1 (i.e., $k_{ex} \approx 1\ s^{-1}$).41 Studying hydrogen exchange processes using the hyperpolarized water principles described in this paper, has many features that complement both of these methods – both due to its real-time nature, and by virtue of the various timescales that the hyperpolarization lifetime enables one to probe. In particular, the fact that a high signal contrast is not governed solely by the intrinsic T_1 of the exchanging sites but rather by $T_1(H_2O)$ (Fig. 3C, bottom), means that it should be possible to characterize slower rates of k_{ex} than in conventional magnetization transfer methods. This intriguing research avenue is currently being investigated.

Supplementary Material

Refer to Web version on PubMed Central for supplementary material.

Acknowledgements

We are grateful to K. Zibzener for technical assistance, and to Dr. Shira Albeck (ISPC, Weizmann Institute) for the preparation of the reductase lysate. Financial support from ERC Advanced Grant #246754, EU'S BioNMR Grant

#261863, DIP Project 710907 (Ministry of Education and Research, Germany), the Clore Foundation, and the generosity of the Perlman Family Foundation, are also acknowledged.

References

(1). Abragam A, Goldman M. Rep Prog Phys. 1978; 41:395.

(2). Wind, RA. eMagRes. John Wiley & Sons Ltd; 2007.

(3). Barnes AB, De Paëpe G, van der Wel PCA, Hu KN, Joo CG, Bajaj VS, Mak-Jurkauskas ML, Sirigiri JR, Herzfeld J, Temkin RJ, Griffin RG. Appl Magn Reson. 2008; 34:237. [PubMed: 19194532]

(4). Maly T, Debelouchina GT, Bajaj VS, Hu K-N, Joo C-G, MakJurkauskas ML, Sirigiri JR, Wel PCAvd, Herzfeld J, Temkin RJ, Griffin RG. J Chem Phys. 2008; 128:052211. [PubMed: 18266416]

(5). Prisner T, Köckenberger W. Appl Magn Reson (special issue). 2008; 34:213.

(6). Griffin RG, Prisner TF. Phys Chem Chem Phys (special issue). 2010; 12:5737.

(7). Bennati, M.; Tkach, I.; Turke, MT. Electron Paramagnetic Resonance: Volume 22. Vol. 22. The Royal Society of Chemistry; 2011. p. 155

(8). Rossini AJ, Zagdoun A, Hegner F, Schwarzwälder M, Gajan D, Copéret C, Lesage A, Emsley L. J Am Chem Soc. 2012; 134:16899. [PubMed: 22967206]

(9). Ardenkjaer-Larsen JH, Fridlund B, Gram A, Hansson G, Hansson L, Lerche MH, Servin R, Thaning M, Golman K. Proc Natl Acad Sci U S A. 2003; 100:10158. [PubMed: 12930897]

(10). Kurhanewicz J, Vigneron DB, Brindle K, Chekmenev EY, Comment A, Cunningham CH, DeBerardinis RJ, Green GG, Leach MO, Rajan SS, Rizi RR, et al. Neoplasia. 2011; 13:81. [PubMed: 21403835]

(11). Wolber J, Ellner F, Fridlund B, Gram A, Jóhannesson H, Hansson G, Hansson LH, Lerche MH, Månsson S, Servin R, Thaning M, et al. Nucl Instrum Methods Phys Res A. 2004; 526:173.

(12). Day SE, Kettunen MI, Gallagher FA, Hu DE, Lerche M, Wolber J, Golman K, Ardenkjaer-Larsen JH, Brindle KM. Nat Med. 2007; 13:1382. [PubMed: 17965722]

(13). Mieville P, Jannin S, Helm L, Bodenhausen G. Chimia. 2011; 65:260. [PubMed: 21678775]

(14). Bornet A, Melzi R, Jannin S, Bodenhausen G. Appl Magn Reson. 2012; 43:107.

(15). Bornet A, Melzi R, Perez Linde AJ, Hautle P, van den Brandt B, Jannin S, Bodenhausen G. J Chem Phys Lett. 2012; 4:111.

(16). Hurd RE, Yen Y-F, Chen A, Ardenkjaer-Larsen JH. J Magn Reson Imaging. 2012; 36:1314. [PubMed: 23165733]

(17). Jannin S, Bornet A, Melzi R, Bodenhausen G. Chem Phys Lett. 2012; 549:99.

(18). Mishkovsky M, Eliav U, Navon G, Frydman L. J Magn Reson. 2009; 200:142. [PubMed: 19574073]

(19). Lerche MH, Meier S, Jensen PR, Hustvedt S-O, Karlsson M, Duus JØ, Ardenkjær-Larsen JH. NMR Biomed. 2011; 24:96. [PubMed: 20862657]

(20). Ragavan M, Chen H-Y, Sekar G, Hilty C. Anal Chem. 2011; 83:6054. [PubMed: 21651293]

(21). Kay LE, Torchia DA, Bax A. Biochemistry. 1989; 28:8972. [PubMed: 2690953]

(22). Yao S, Babon JJ, Norton RS. Biophys Chem. 2008; 136:145. [PubMed: 18583018]

(23). Ferrage F, Dutta K, Shekhtman A, Cowburn D. J Biomol NMR. 2010; 47:41. [PubMed: 20372977]

(24). Leggett J, Hunter R, Granwehr J, Panek R, Perez-Linde AJ, Horsewill AJ, McMaster J, Smith G, Kockenberger W. Phys Chem Chem Phys. 2010; 12:5883. [PubMed: 20458428]

(25). Bowen S, Hilty C. Angew Chem Int Ed. 2008; 47:5235.

(26). Bowen S, Hilty C. Phys Chem Chem Phys. 2010; 12:5766. [PubMed: 20442947]

(27). Barb AW, Hekmatyar SK, Glushka JN, Prestegard JH. J Magn Reson. 2011; 212:304. [PubMed: 21824795]

(28). Massiot D, Fayon F, Capron M, King I, Le Calvé S, Alonso B, Durand J-O, Bujoli B, Gan Z, Hoatson G. Magn Reson Chem. 2002; 40:70.

(29). Ardenkjaer-Larsen, JH.; Laustsen, C.; Pullinger, B.; Kadlecek, S.; Emami, K.; Rizi, R. Proc Intl Soc Mag Reson Med 19. Montreal: 2011. p. 3534
(30). Harris T, Bretschneider C, Frydman L. J Magn Reson. 2011; 211:96. [PubMed: 21531156]
(31). Polnaszek CF, Bryant RG. J Chem Phys. 1984; 81:4038.
(32). Bennati M, Luchinat C, Parigi G, Turke M-T. Phys Chem Chem Phys. 2010; 12:5902. [PubMed: 20458388]
(33). McCarney ER, Armstrong BD, Lingwood MD, Han S. Proc Natl Acad Sci USA. 2007; 104:1754. [PubMed: 17264210]
(34). McConnell HM. J Chem Phys. 1958; 28:430.
(35). Henry GD, Sykes BD. J Biomol NMR. 1995; 6:59. [PubMed: 22911578]
(36). Liepinsh E, Otting G. Magn Reson Med. 1996; 35:30. [PubMed: 8771020]
(37). Krishna NR, Goldstein G, Glickson JD. Biopolymers. 1980; 19:2003. [PubMed: 7437500]
(38). Armstrong BD, Han S. J Am Chem Soc. 2009; 131:4641. [PubMed: 19290661]
(39). Englander SW, Mayne L. Annu Rev Biophys Biomol Struct. 1992; 21:243. [PubMed: 1525469]
(40). Englander SW. Annu Rev Biophys Biomol Struct. 2000; 29:213. [PubMed: 10940248]
(41). Waelder S, Lee L, Redfield AG. J Am Chem Soc. 1975; 97:2927. [PubMed: 1133343]

Europe PMC Funders Author Manuscripts

Europe PMC Funders Author Manuscripts

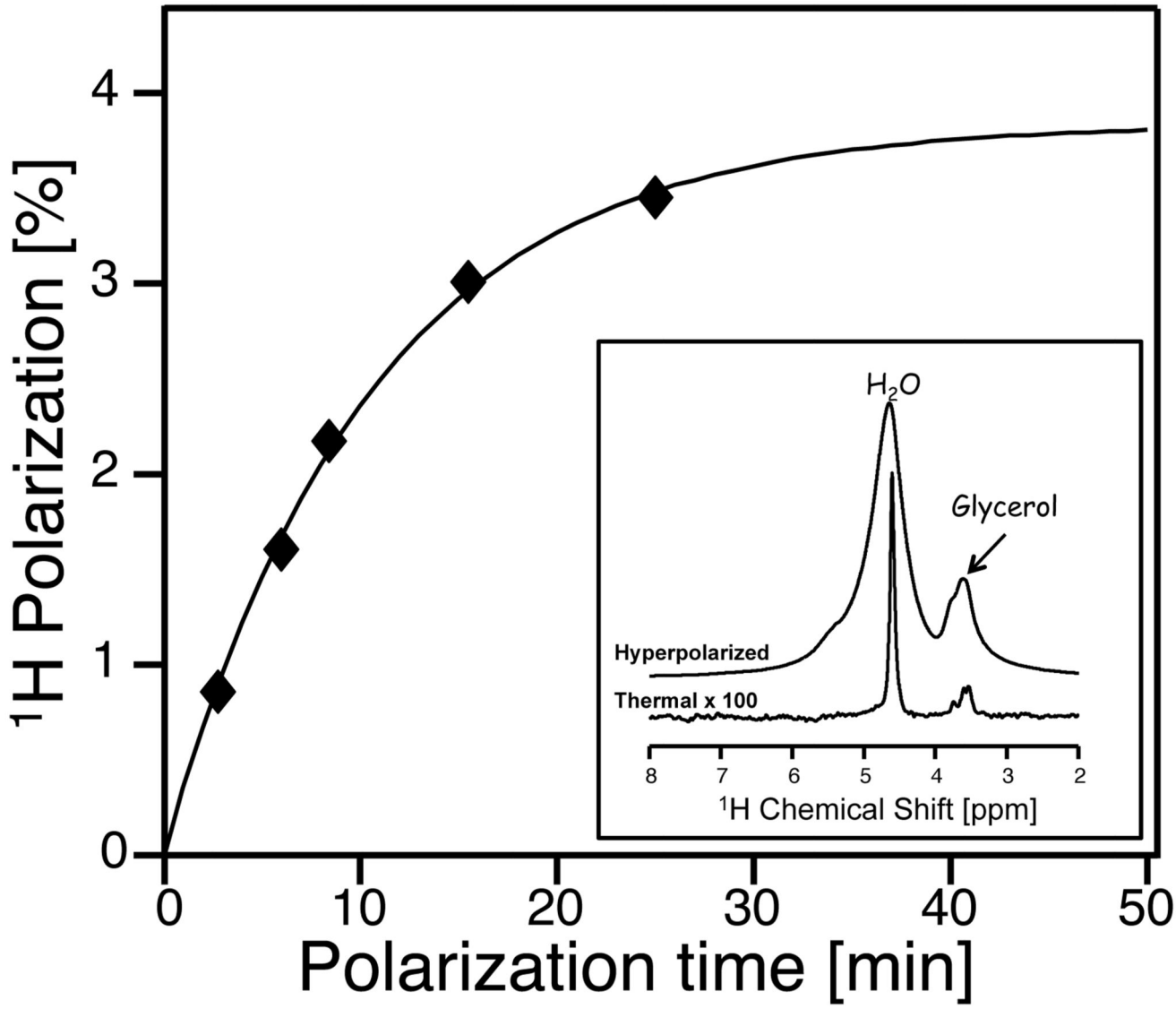

Figure 1.

DNP-enhanced ^{1}H signal buildup observed for water, as a function of the polarization time under cryogenic conditions. The experimental points arise from independent dissolution experiments, where the water signal enhancement was compared to the thermal counterpart after returning to equilibrium. Samples consisted of 30 μL H_2O:Glycerol 3:2 (v/v) hyperpolarized at 1.5 K and 94.1 GHz using 25 mM TEMPO as polarizing agent, and subsequently dissolved with 3 mL D_2O. Comparison of the resulting data to its thermal counterpart (inset) indicates a plateauing ^{1}H polarization at these conditions of (3.9±0.3)% and a buildup time constant of (10±2) min. Alternative polarization and dissolution conditions (cf. Fig. 2) can elevate the former figure beyond 5 %.

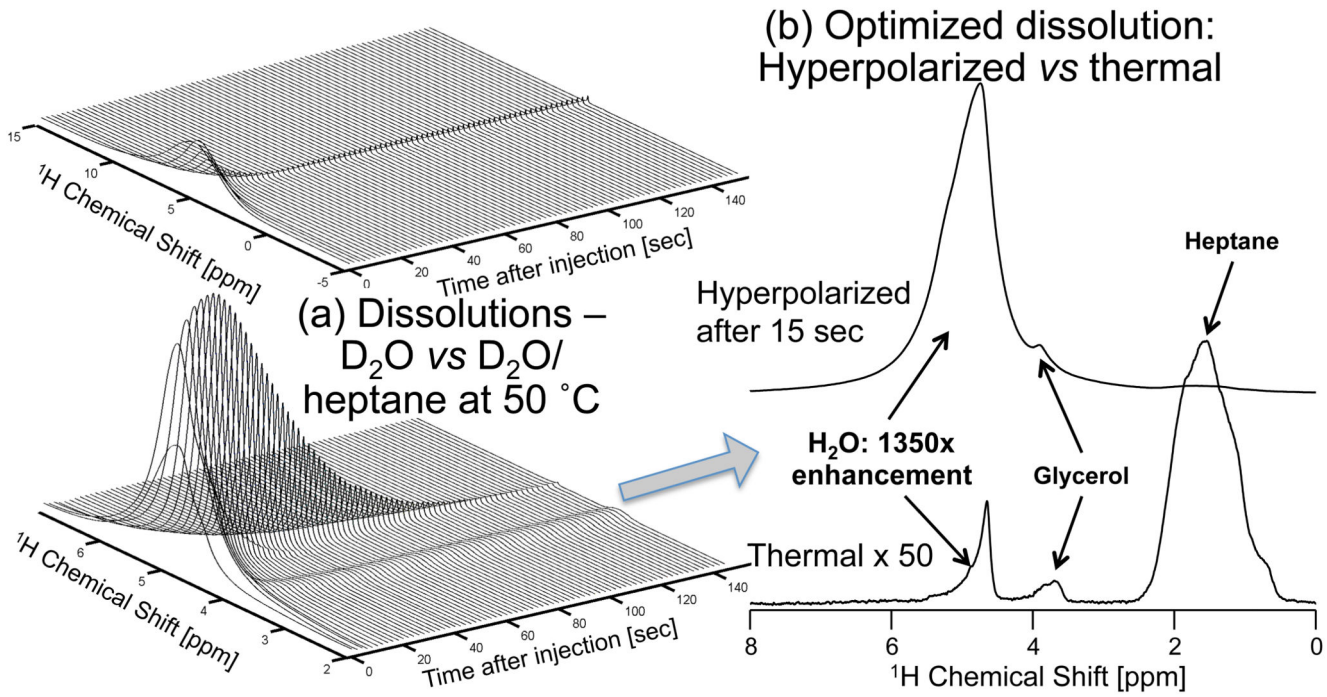

Figure 2.

Improving water's hyperpolarized signal by co-dissolution with heptane. (a) Water signal evolution following hyperpolarization of a 150 μL 3:2 (v/v) mixture of H_2O:Glycerol with 25 mM TEMPO, and dissolution in either 3 mL at ~35°C D_2O (top), or in a mixture of 1.5 mL D_2O and 3mL heptane with transport and measurement at ca. 50°C (bottom). The relaxation time T_1 of the water resonance is extended from 3.6 sec (top) to 18.2 sec (bottom), and the absolute enhancement at t = 0 is increased by a factor of 4.5. (b) Comparison between the hyperpolarized 1D ^{1}H NMR arising from the D_2O/heptane dissolution 15 seconds after it has reached the NMR magnet, and a thermal spectrum of the same sample. All spectra were obtained by acquiring 28 k complex data points using a small (~1°) flip-angle pulse excitation and a carrier frequency set to 2.9 ppm; time zero corresponds to the conclusion of the sample flushing from the DNP polarizer.

Europe PMC Funders Author Manuscripts

Europe PMC Funders Author Manuscripts

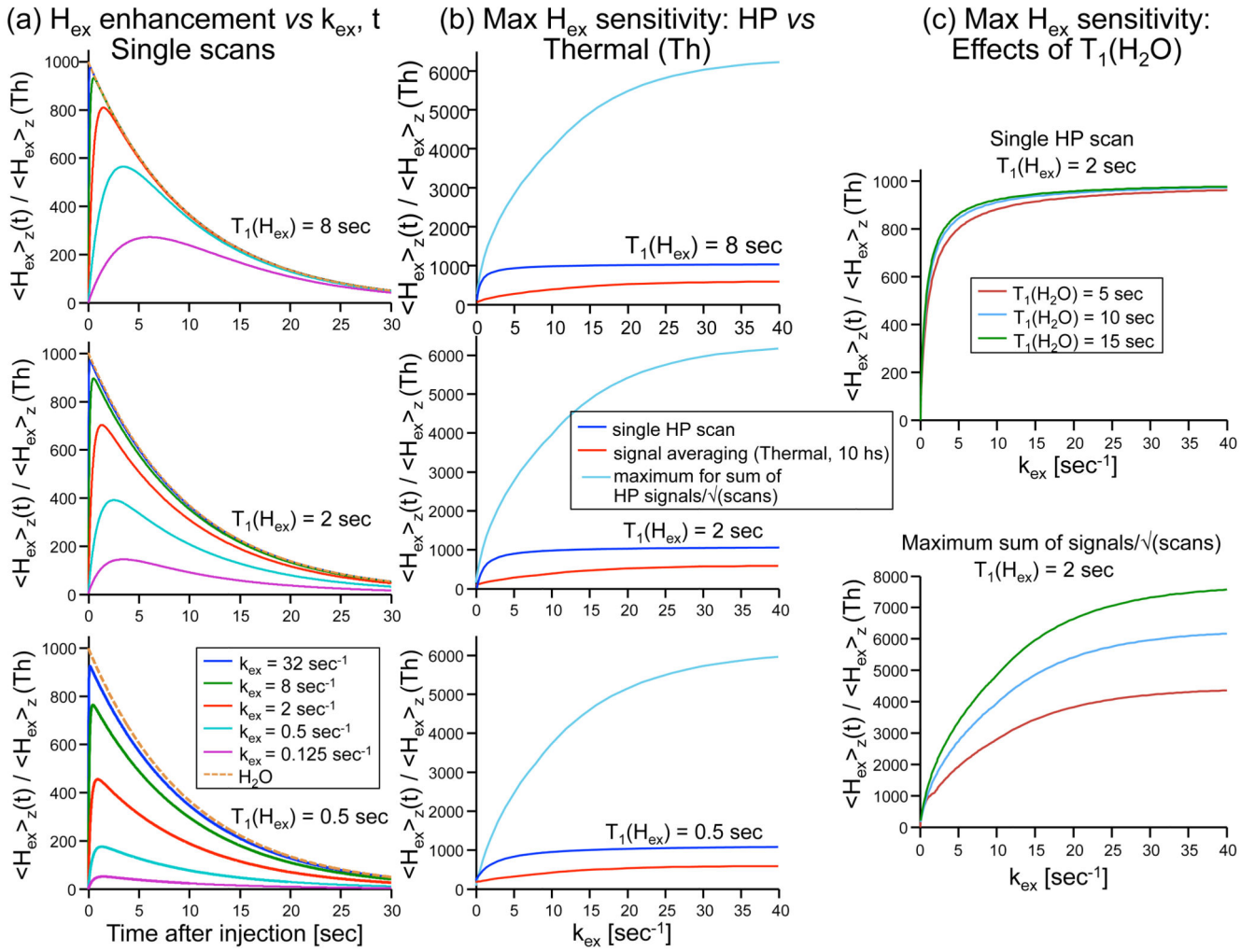

Figure 3.

Calculations of the relative ^{1}H magnetization enhancements of protons H_{ex}, due to exchange with hyperpolarized water protons. Unless stated otherwise the relaxation of water was kept constant at $T_1^{H_2O}$ = 10 sec, and the initial relative enhancement of water was $\langle H_2O\rangle_z(0)/\langle H_2O\rangle_z(\mathrm{Th}) = 1000$. (a) Enhancement as a function of time since the hyperpolarized (HP) water injection, for the different exchange rate(k_{ex}) values indicated in the bottom panel. Calculations are given for three different values of $T_1(H_{ex})$ (top, middle and bottom panels); the dashed orange line in all panels represents the decay of the water polarization with time. (b) Enhancement achievable by H_{ex} as a function of k_{ex}, calculated assuming that: a single scan was measured by a 90° pulse at an optimal time after injection of hyperpolarized water (blue lines), that thermal signal averaging was performed over the course of 10 hours with optimal conditions (ie., with 90° pulses and recycle delays given by k_{ex} and not solely by $T_1(H_{ex})$; red lines), or that multiple hyperpolarized scans were done on H_{ex} at optimum times assuming minimal TR of 100 ms (cyan lines; in this latter case we display the sum of signals collected with 90° pulses divided by square root of the number of scans). Other parameters are the same as in (a). (c) The effect of $T_1(H_2O)$ on the H_{ex}

enhancement, shown for an optimized single scan acquisition (top), or for multiple scans seeking maximum SNR as a function of k_{ex}. $T_1(H_{ex})$ = 2 sec and the $T_1(H_2O)$ is varied – 5, 10 and 15 sec (red, cyan and green lines, respectively).

Europe PMC Funders Author Manuscripts

Europe PMC Funders Author Manuscripts

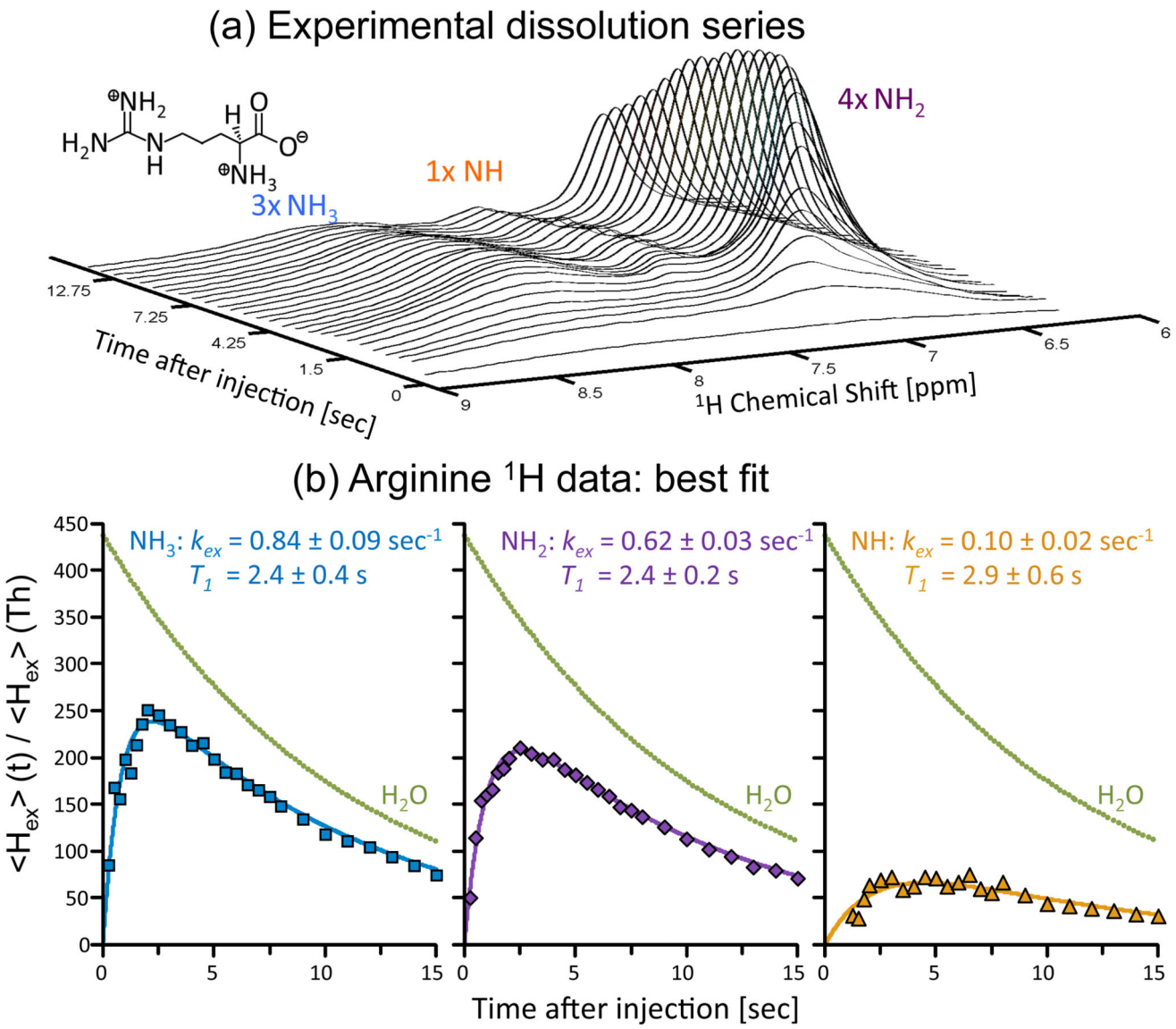

Figure 4.

Transferring water hyperpolarization to the resonance of arginine's exchangeable protons. (a) Progression of arginine's ^{1}H NMR spectrum upon sudden dissolution of hyperpolarized water into 3 mL of a 1M arginine sample (pD ~ 3) dissolved in D_2O, and waiting in the 500 MHz spectrometer used to collect the data. Each trace involved the acquisition of 4k complex points, arising from a small flip-angle (~1°) excitation (carrier at 7.3 ppm) with a 0.25 sec TR. The different types of protons in the arginine sample (inset - molecular formula) are indicated above their corresponding peaks. (b) Peak intensities arising from the experimental time course, together with fits to Eq. (2) for each arginine site (solid lines), lead to the indicated relaxation times T_1 and exchange rates k_{ex}. These fits revealed an initial water polarization enhancement of (438±3)×, and a characteristic decay $T_1(H_2O)$ of 10.9 ± 0.1 sec; the ensuing decay curve is presented in the figure as green dots).

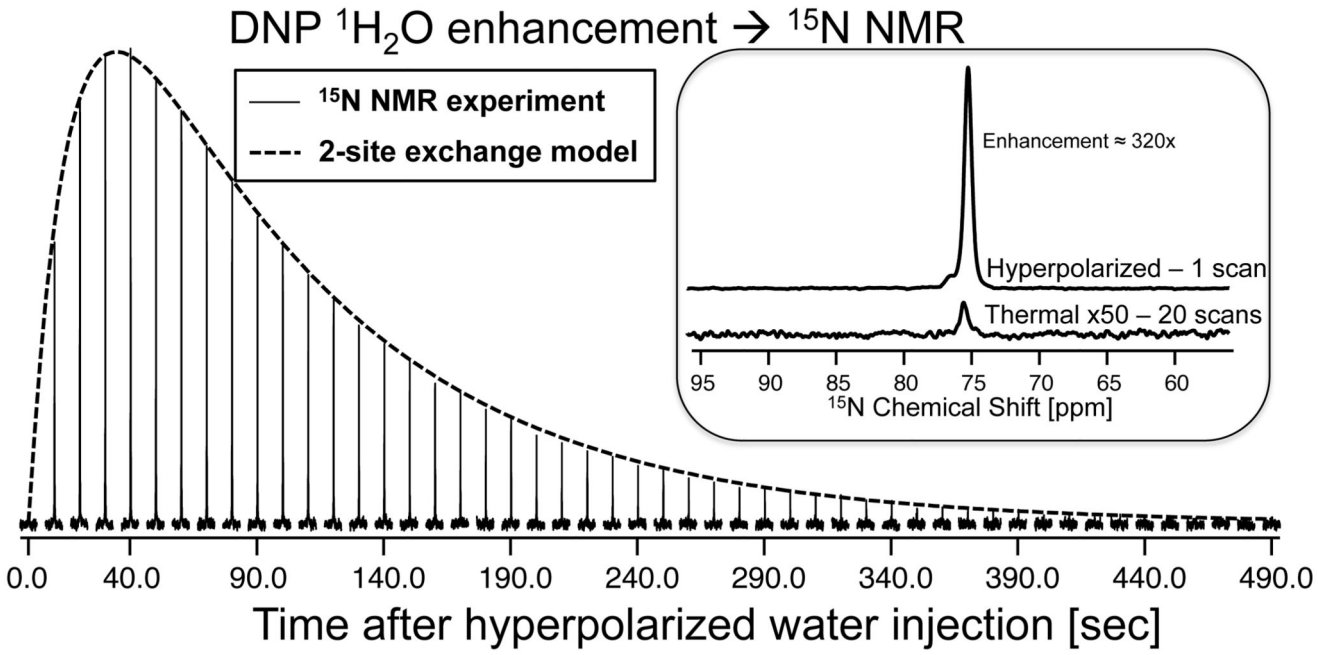

Figure 5.

^{15}N NMR enhancement achieved in ^{15}N-urea via heteronuclear polarization transfer from hyperpolarized water. Spectra were collected using a small flip-angle (9°) single-pulse irradiating on the ^{15}N channel at 76 ppm, and acquiring 9 k data points (4 sec acquisition time). The dashed line is a fit to the two-site exchange model in eq. (3). The inset compares a single-scan DNP-enhanced ^{15}N spectrum collected using a 90° pulse applied at an optimal post-injection delay of ≈40 sec, against a thermal equilibrium ^{15}N NMR spectrum measured for the same sample by signal averaging 20 fully-relaxed scans, over a total of 13:50 hours. All measurements were done at 50 °C.

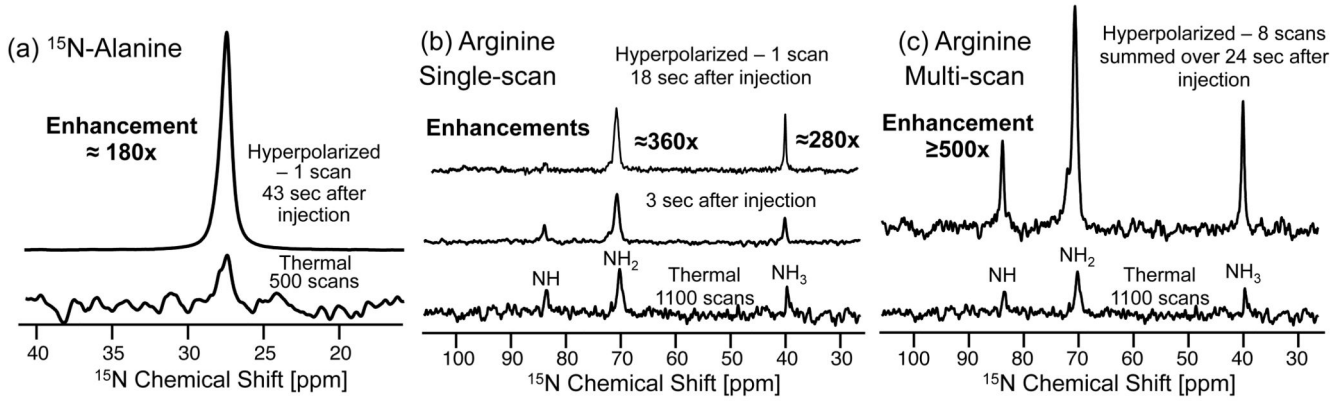

Figure 6.

Enhancement vis-à-vis thermal counterparts of the ^{15}N signals of ^{15}N-alanine (a) and of natural abundance arginine ((b) and (c)), by polarization transfers from hyperpolarized water. The optimal delay in each case was extracted from simulations of the kind given in Figure 5. Hyperpolarized ^{15}N NMR spectra in (a) and (b) were detected in single-scan experiments using a 90° ^{15}N pulse, applied 43 and 18 sec after the injection of the water, respectively. Thermal acquisitions in (a) and (b/c) took ca. 2 and 14 hours, respectively. (c) Sum of the first 8 scans collected after injection of hyperpolarized water to an arginine sample, over a total time of 24 sec. An effective average enhancement ≥500× is observed. All measurements were done at ≈50 °C under conditions akin to those in Fig. 5. Notice that the **N**H of arginine has significantly lower enhancement than the other two peaks due to its slow k_{ex} at pH≈3.

Europe PMC Funders Author Manuscripts

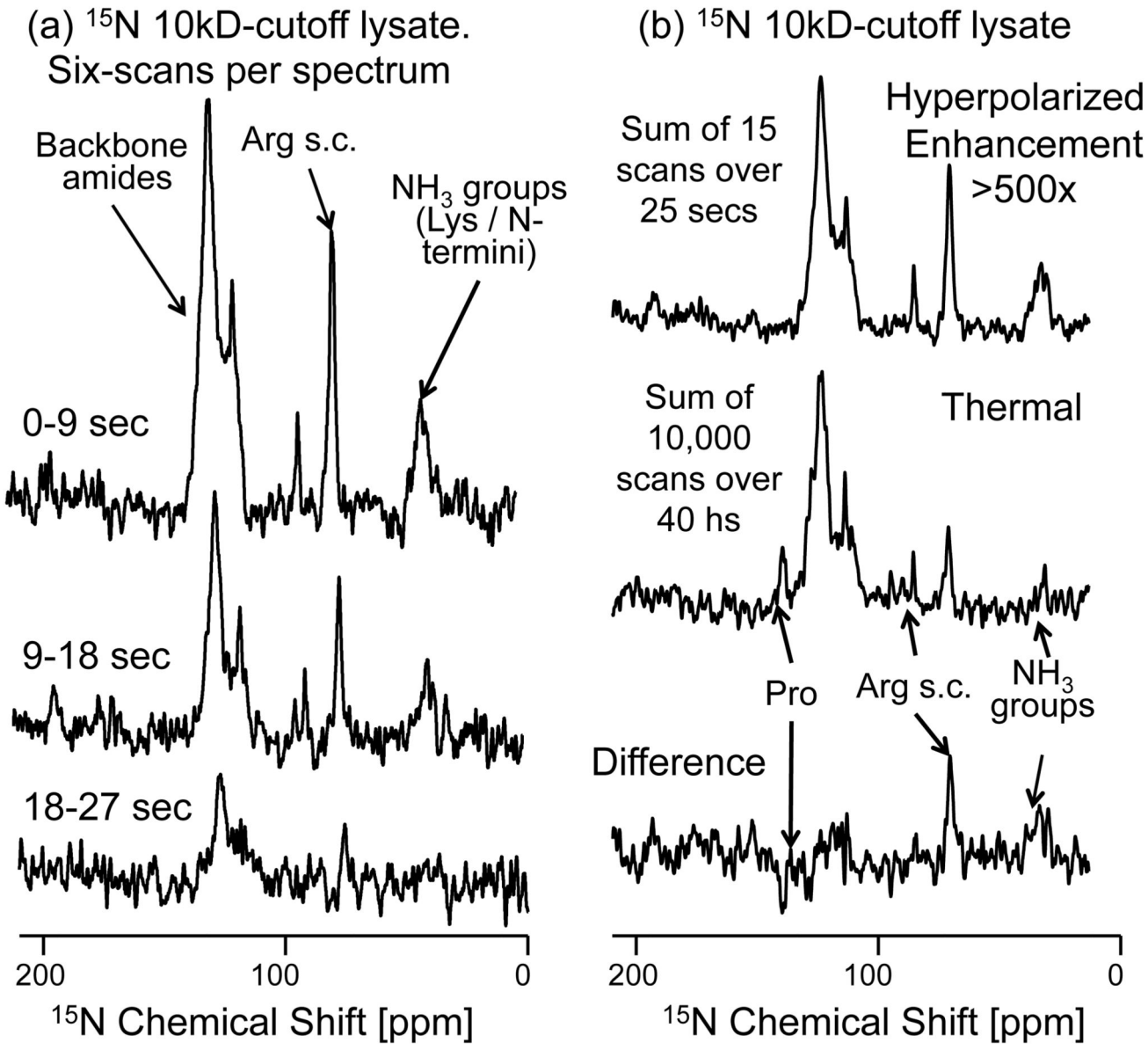

Figure 7.

Enhancement of ^{15}N signals in a ^{15}N-labeled polypeptide lysate with molecular weight cut-off of 10kDa, via polarization transfer from hyperpolarized water. (a) ^{15}N NMR spectra arising from 90° ^{15}N pulses applied over the indicated post-dissolution times, reflecting the 17.9 sec T_1 we detect for the water protons onto the ^{15}N signals enhanced by the exchangeable protons. The sum of six consecutive scans from this time series are displayed. (b) Sum of first 15 scans (upper trace) following the injection of hyperpolarized water, compared *vs* a thermal equilibrium ^{15}N spectrum (middle trace), measured by signal averaging 10000 scans over the course of ca. 40 hours. The difference between these spectra is displayed in the bottom trace, highlighting the over-enhancement of the arginine side-chains (NH_2) and lysine's (NH_3) groups, and the under-enhancement of the proton-less

proline backbone nitrogens. The average signal enhancement of the ^{15}N backbone amides is >500× relative to ^{15}N thermal equilibrium signal. Other acquisition parameters are as in Figure 5.

Europe PMC Funders Author Manuscripts